Resonance-fluorescence-localization microscopy with subwavelength resolution

Zeyang Liao,[1] M. Al-Amri,[2] and M. Suhail Zubairy[1]

[1]*Department of Physics and Astronomy, Institute for Quantum Studies, Texas A&M University, College Station, Texas 77843-4242, USA*

[2]*The National Center for Mathematics and Physics, KACST, P.O. Box 6086, Riyadh 11442, Saudi Arabia*

(Received 9 July 2011; revised manuscript received 23 November 2011; published 9 February 2012)

We evaluate the resonance-fluorescence spectrum of a bunch of two-level atoms driven by a gradient coherent laser field. The result shows that we can determine the positions of atoms from the spectrum even when the atoms locate within the subwavelength range and the dipole-dipole interaction is significant. This far-field resonance-fluorescence-localization microscopy method does not require point-by-point scanning, and it may be more time efficient. We also give a possible scheme to extract the position information in an extended region without requiring more peak power of the laser. Finally, we also briefly discuss how to perform two-dimensional imaging based on our scheme.

DOI: 10.1103/PhysRevA.85.023810 PACS number(s): 42.30.−d, 42.50.Hz, 42.62.Fi

I. INTRODUCTION

The resolution limit of traditional far-field optical microscopy is about a half wavelength of the light [1,2]. To get a better resolution, one has to switch to a shorter wavelength (e.g., electron microscope), which usually is invasive to the system [3]. Near-field scanning microscopy can obtain an optical imaging with subdiffraction resolution [4,5], but due to the surface-bound nature, it is limited in application. Two-photon fluorescence microscopy first was developed to achieve a higher resolution than classical one-photon fluorescence microscopy in the far field [6,7]. Stimulated emission depletion and the related concept of ground-state depletion microscopy then were developed to overcome the far-field diffraction limit in fluorescence microscopy [8–11]. Space-dependent dark states also were proposed to achieve subwavelength resolution [12–17]. However, realization of these schemes is based on point-by-point scanning, and it is time consuming. Coherent Rabi oscillations also can be employed to break the diffraction limit [18–20], but the effect of dipole-dipole interaction has not been discussed well. Another method based on resonance fluorescence is able to measure the separation of two interacting atoms with a subwavelength resolution [21,22].

The question remains whether we can determine the locations of multiple atoms with subwavelength resolution even when dipole-dipole interaction is involved. In this paper, we demonstrate that the collective resonance fluorescence can provide the spatial information for a multiatom system, and we can perform a far-field resonance-fluorescence-localization microscopy (RFLM) with a subwavelength resolution.

This paper is organized as follows. In Sec. II, we evaluate the general spectrum formalism for N interacting atoms and illustrate how to extract position information from the spectrum. In Sec. III, we numerically solve a three-atom example without approximation to show that our method, illustrated in Sec. II, works. In Sec. IV, we show how to image a sample with a large area using just a few measurements and without needing more peak power of the laser field. We also briefly show how to image a sample in a two-dimensional (2D) region. In Sec. V, we summarize our results. Finally, calculations of eigenvalues and eigenvectors are given in Appendix A, whereas, the linewidth evaluation is given in Appendix B.

II. GENERAL FORMALISM FOR N ATOMS RFLM

For simplicity, we first consider that some identical atoms are located in a line along the x axis. Our setup is shown in Fig. 1. We shine two strong linear-polarized laser fields with wavelength λ on these atoms from opposite directions, and they form a standing wave. Assume that the polarization orientation is in the $\hat{y}$ direction, and the frequency is resonant with the two-level atoms. We also assume that the atoms do not move, and they locate within one wavelength. This assumption is valid for the following situations: Atoms are trapped by optical lattices, quantum dots, and nitrogen-vacancy centers in diamond, and so on. We can stretch the standing wave where the sample approximately is located within the linear region between the node and the antinode [15,18]. In this region, we can write $E(x) = E_0 x/\lambda$. We monitor the resonance-fluorescence photons emitted by the system with a detector in the $\hat{z}$ direction. The resonance-fluorescence spectrum encodes the spatial information of the systems from which we can determine the positions of each atom.

The Hamiltonian of the system and the field is [21,23]

$$H = H_A + H_F + H_{AF} + H_{dd}, \tag{1}$$

where $H_A = \hbar\omega_0 \sum_{i=1}^{N} S_i^z$ is the energy of the atoms, with ω_0 being the level separation and S_i^z is the z component of the spin operator. $H_F = \hbar\omega_0 a^\dagger a$ is the total energy of the photons, where $a(a^\dagger)$ is the annihilation (creation) operator of the photon; $H_{AF} = (\hbar/2)\sum_{i=1}^{N} g_i(S_i^+ a + S_i^- a^\dagger)$ is the interaction between the atoms and the field with $S_i^+(S_i^-)$ being the raising (lowering) operator on the ith atom and the coupling constants $g_i = g x_i/\lambda$ and $g = \mu(2\omega_0/\hbar\varepsilon_0 V)^{1/2}$ (μ is the transition-dipole moment between ground state and excited state); $H_{dd} = \hbar\sum_{i\neq j}\Omega_{ij}(S_i^+ S_j^- + S_i^- S_j^+)$ is the dipole-dipole interaction energy. All transition-dipole moments are polarized in the y direction, and the dipole-dipole interaction energy Ω_{ij} is given by [21–23]

$$\Omega_{ij} = \frac{3\gamma}{4}\left[-\frac{\cos(kx_{ij})}{kx_{ij}} + \frac{\sin(kx_{ij})}{(kx_{ij})^2} + \frac{\cos(kx_{ij})}{(kx_{ij})^3}\right], \tag{2}$$

with $2\gamma = 4\omega_0^3 d_0^2/(3\hbar c^3)$ being the single-atom spontaneous decay rate, $k = \omega_0/c$ (c is the speed of light), and x_{ij} is the distance between atoms [23–25]. The Rabi frequency for the

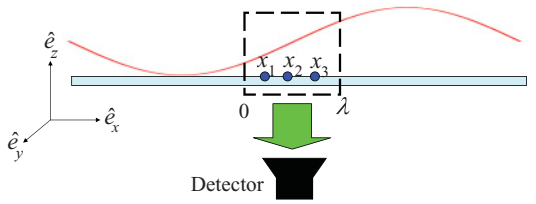

FIG. 1. (Color online) Scheme for resonance-fluorescence microscopy. x_i is the position of the ith atom.

ith atom is given by $\Omega_i = g_i\sqrt{n}$ (or $\mu E_0 x_i/\hbar\lambda$), where n is the photon number.

A. $\Omega_i \gg \Omega_{ij}$

If the dipole-dipole interaction energy is not very strong, we can apply a strong laser field such that $\Omega_i \gg \Omega_{ij}$. In this case, we analytically can evaluate the collective resonance fluorescence spectrum of the multiatom system based on a dressed-state picture [26,27]. Let $H_0 = H_A + H_F + H_{AF}$, and treat H_{dd} as a perturbation term. The eigenvalues and eigenfunctions of H_0 are given by (Appendix A)

$$E^0_{\alpha,n} = \left(n - \frac{N}{2}\right)\hbar\omega_0 + \frac{\hbar}{2}\sum_{i=1}^{N}\chi_i^\alpha\Omega_i, \tag{3}$$

$$|\alpha,n\rangle = \frac{1}{\sqrt{2^N}}\Bigg(|b^N,n\rangle + \sum_{i=1}^{N}\chi_i^\alpha|a_i b^{N-1},n-1\rangle + \sum_{i\neq j}\chi_i^\alpha\chi_j^\alpha|a_i a_j b^{N-2},n-2\rangle + \cdots + \prod_{i=1}^{N}\chi_i^\alpha|a^N,n-N\rangle\Bigg), \tag{4}$$

where N is the number of atoms, $\alpha = 1,2,\ldots,2^N$, $|a_i b^{N-1}\rangle$ means that the ith atom is in the excited state $|a\rangle$ while other $N-1$ atoms are in the ground state $|b\rangle$ and χ_i^α is a constant that can be either $+1$ or -1. Counting the dipole-dipole interaction term as a perturbation, the eigenenergy is shifted by

$$\Delta_{\alpha,n} = \frac{\hbar}{2}\sum_{i\neq j}\chi_i^\alpha\chi_j^\alpha\Omega_{ij}, \tag{5}$$

and the correction to the zeroth-order eigenfunction is on the order of Ω_{ij}/Ω_i, which can be neglected. The sublevel energy is $E_{\alpha,n} = E^0_{\alpha,n} + \Delta_{\alpha,n}$. The pictorial energy level for the dressed-state picture is shown in Fig. 2. Coupling of the dressed states to the vacuum results in the system's cascade down the ladder from the α state of one multiplet to the β state of the adjacent multiplet [26]. The corresponding transition frequency is $\omega_{\alpha\beta} = (E_{\alpha,n} - E_{\beta,n-1})/\hbar$, where $\alpha,\beta = 1,2,\ldots,2^N$.

The spectrum of resonance fluorescence can be evaluated by [26,27]

$$S(\omega) \propto \mathrm{Re}\left[\int_0^\infty d\tau\, e^{i\omega\tau}\lim_{t\to\infty}\langle D^+(t)D^-(t+\tau)\rangle\right], \tag{6}$$

where D^+ and D^- are the raising and lowering parts of the total atomic-dipole operator. The lowering part can be written as

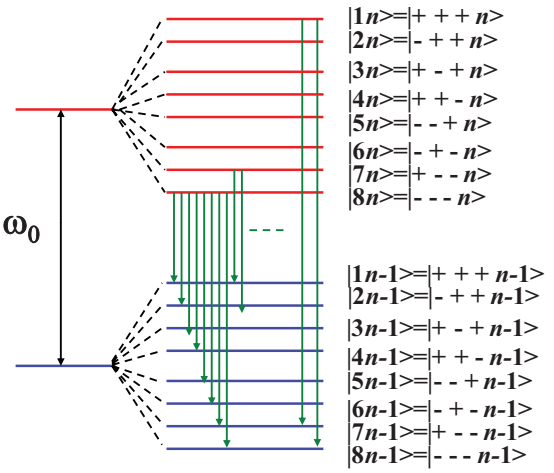

FIG. 2. (Color online) Dressed-state picture for three interacting atoms. $|\pm\pm\pm n\rangle = (|bn_1\rangle \pm |an_1-1\rangle)\otimes(|bn_2\rangle \pm |an_2-1\rangle)\otimes(|bn_3\rangle \pm |an_3-1\rangle)$ where $n_1+n_2+n_3 = n$.

$D^- = \sum_{\alpha\beta n} d^-_{\alpha\beta}|\beta,n-1\rangle\langle\alpha,n| = \sum_{\alpha\beta} D^-_{\alpha\beta}$, where $d^-_{\alpha\beta}$ is the dipole matrix element of the transition from $|\alpha,n\rangle$ to $|\beta,n-1\rangle$ and it is defined by $d^-_{\alpha\beta} = \langle\beta,n-1|\sum_{i=1}^N S_i^-|\alpha,n\rangle$ and $D^-_{\alpha\beta} = \sum_n d^-_{\alpha\beta}|\beta,n-1\rangle\langle\alpha,n|$.

We can write the two-time correlation function in Eq. (6) as

$$\langle D^+(t)D^-(t+\tau)\rangle = \sum_{\alpha\neq\beta}\langle D^+(t)D^-_{\alpha\beta}(t+\tau)\rangle + \sum_{\alpha}\langle D^+(t)D^-_{\alpha\alpha}(t+\tau)\rangle, \tag{7}$$

where the first term corresponds to the sideband spectrum while the second term corresponds to the central peak. According to the quantum-regression theorem [28], the two-time correlation function $\langle D^+(t)D^-_{\alpha\beta}(t+\tau)\rangle$ satisfies the same equation of motion as the single-time average $\langle D^-_{\alpha\beta}(t)\rangle$. The dynamics of $\langle D^-_{\alpha\beta}(t)\rangle$ can be calculated from the master equation,

$$\frac{d\langle D^-_{\alpha\beta}(t)\rangle}{dt} = d^-_{\alpha\beta}\frac{d\rho^-_{\alpha\beta}}{dt} = d^-_{\alpha\beta}\left\{\frac{-i}{\hbar}[H,\rho]_{\alpha\beta} - (L\rho)_{\alpha\beta}\right\}, \tag{8}$$

where $\rho^-_{\alpha\beta} = \langle\alpha,n|\rho|\beta,n-1\rangle$, and $L = \sum_{i,j=1}^N\gamma_{ij}(S_i^+S_j^-\rho + \rho S_i^+S_j^- - 2S_j^-\rho S_i^+)$ is the relaxation operator with γ_{ii} being the decay rate of atom i and γ_{ij} being the cross-damping rate. For the sidebands, we can expand $(L\rho)_{\alpha\beta} = \Gamma_{\alpha\beta}\rho_{\alpha\beta} + \cdots$ and, from Eq. (8), we have

$$\frac{d}{dt}\langle D^-_{\alpha\beta}(t)\rangle \simeq (i\omega_{\alpha\beta} - \Gamma_{\alpha\beta})\langle D^-_{\alpha\beta}(t)\rangle, \tag{9}$$

where we have neglected the nonresonance terms on the right-hand side in the secular approximation. For the central peak, as all $|\alpha,n\rangle \to |\alpha,n-1\rangle$, $\alpha = 1,\ldots,2^N$ have the same transition frequency, they couple to each other, and we can expand $(L\rho)_{\alpha\alpha} = \sum_\beta\Gamma'_{\alpha\beta}\rho_{\beta\beta} + \cdots$. From Eq. (8), we get

$$\frac{d}{dt}\langle D^-_{\alpha\alpha}(t)\rangle = i\omega_0\langle D^-_{\alpha\alpha}(t)\rangle - d^-_{\alpha\alpha}\sum_\beta\Gamma'_{\alpha\beta}\frac{\langle D^-_{\beta\beta}(t)\rangle}{d^-_{\beta\beta}}. \tag{10}$$

According to the quantum-regression theorem and Eq. (6), the spectrum is given by

$$S(\vec{R},\omega) = S^0(\omega) + S^{\pm}(\omega) \propto \mathrm{Re}\left[\int_0^\infty d\tau\, e^{i(\omega-\omega_0)\tau} \sum_{\alpha,\beta} d^-_{\alpha\alpha}(e^{-\Gamma'\tau})_{\alpha\beta} d^+_{\beta\beta}\right] + \sum_{\alpha\neq\beta} \frac{|d^-_{\alpha\beta}|^2\Gamma_{\alpha\beta}}{(\omega-\omega_{\alpha\beta})^2+\Gamma^2_{\alpha\beta}}, \tag{11}$$

where the first term yields the central peak spectrum and the second term gives the sideband spectrum.

For the zeroth-order wave function [Eq. (4) or, equivalently, Eq. (A1)], the transition dipole is given by

$$d^-_{\alpha\beta} = \frac{1}{2^N}\sum_{i=1}^{N}\left\{\chi_i^\beta \prod_{k\neq i}\left[1+\chi_k^\alpha\chi_k^\beta\right]\right\}. \tag{12}$$

We have three cases:

(1) $\beta=\alpha$, $d^-_{\alpha\beta} = \sum_{i=1}^N \chi_i^\alpha/2$, which contributes to the central peak $\omega=\omega_0$;

(2) $\beta=\alpha^p$ (α^p is a state such that E^0_α and $E^0_{\alpha^p}$ have different signs only in the pth term), $d^-_{\alpha\beta}=\chi_p^\alpha/2$, which contributes to the sidebands,

$$\omega_{\alpha\alpha^p} = \omega_0 + \chi_p^\alpha\Omega_p + \sum_{k\neq p}\chi_p^\alpha\chi_k^\alpha\Omega_{pk}. \tag{13}$$

From this equation, we see that the positive sideband peaks can be divided into N groups: $\Omega_p + \sum_{k\neq p}\pm\Omega_{pk}$, $p=1,\ldots,N$. Averaging over the frequencies of each group, we can get the Rabi frequencies Ω_p from which we can determine the positions of the atoms. The error is on the order of $\Omega_{ij}^2/\Omega_i^2 \ll 1$. This is our method for optical microscopy. In the experiment, we may not know which peak belongs to which group. However, if we change the gradient of the laser field by a certain amount, the relative Rabi frequencies for different atoms change, which causes the separations between different groups of the spectrum shift. Because the dipole-dipole interactions do not change, the splitting between peaks belonging to the same group will not change. From this phenomenon, we can identify peaks belonging to different groups.

(3) $\alpha\neq\beta$ and more than one term of E^0_α and E^0_β have different signs, $d^-_{\alpha\beta}=0$, which corresponds to the forbidden transition.

The method described above is valid under the conditions $\Omega_i \gg \Omega_{ij}$ and $|\Omega_i-\Omega_j|-2\Omega_{ij}\gg\gamma$. Assuming that $\gamma\sim 10^8$ Hz and the maximum Rabi frequency is 10^{13} Hz, then the smallest distance we can resolve in this method is about $\lambda/50$.

B. $\Omega_{ij} \gg \Omega_i$

When there are two atoms in the sample whose distances are very close (e.g., $r_{ij}<\lambda/50$), the condition $\Omega_i\gg\Omega_{ij}$ cannot be satisfied. We cannot localize the positions of these two atoms based on the method described in the previous subsection. However, we still have some ways to extract the position information of the two atoms if they are far away from other atoms (e.g., larger than $\lambda/10$). In this case, we apply a weak gradient field such that $\Omega_i,\Omega_j \ll \Omega_{ij}$. If the Rabi frequency is $\Omega_i\sim\gamma$, there are only two sideband peaks located at $\omega_0\pm\Omega_{ij}$ [21,23]. Therefore, from the resonance-fluorescence spectrum, we can determine the dipole-dipole interaction energy Ω_{ij}. According to Eq. (2), we then can determine the distance r_{ij} between these two close atoms.

Then, we increase the gradient-field strength to a medium value (for example, $\sim 100\gamma$), which still is much less than the dipole-dipole interaction energy. In this case, each sideband peak is split into two peaks [21,23]. For the positive sideband, it splits into two peaks,

$$\omega^1_+ = \omega_0 + \Omega_{ij} + \frac{(\Omega_i+\Omega_j)^2}{2\Omega_{ij}}, \tag{14}$$

$$\omega^2_+ = \omega_0 + \Omega_{ij} + \frac{\Omega_i\Omega_j}{\Omega_{ij}}. \tag{15}$$

From each equation and the relationship between Ω_i and Ω_j, we can calculate a value for positions r_i and r_j. Because we have two equations, we can get two results. We can use one of the results as the positions of the two atoms, or we can average the two results and get the positions of the two atoms.

C. Linewidth

In general, the linewidth of the emitted radiation is difficult to calculate exactly. However, we can evaluate the linewidth approximately in some cases (Appendix B). From Eq. (2), when the distance between two atoms is about $\lambda/10$, the dipole-dipole interaction energy is comparable to the linewidth of the sideband spectrum of the independent atoms. Therefore, we can set $\lambda/10$ as a threshold and can evaluate the linewidth. First, when all the atoms have distances much larger than $\lambda/10$, the dipole-dipole interaction energies are much smaller than the sideband spectrum linewidth of the independent atoms, and we can neglect the dipole-dipole interaction energies. For independent atoms, the linewidth of the sideband spectrum is $3\gamma/2$ [27,28], i.e., $\Gamma_{\alpha\beta}=3\gamma/2$ in Eq. (11). Second, when all the atoms have distances much smaller than $\lambda/10$, all dipole-dipole interaction energies Ω_{ij} are larger than $3\gamma/2$, and the overlapped sideband spectrum splits. We can calculate $(L\rho)_{\alpha\beta}\approx(N/2+1)\gamma\rho_{\alpha\beta}+\cdots$, from which we can see that $\Gamma_{\alpha\beta}\approx(N/2+1)\gamma$ (See Appendix B). The spectrum width is about $(N/2+1)\gamma$, which is similar to super-radiance [29].

For the general case when some atoms have distances larger than $\lambda/10$ and some atoms have distances smaller than $\lambda/10$, the resonance fluorescence has the same transition frequencies but has different linewidths, which are about $(N_{eff}+2)\gamma/2$ where N_{eff} is the average number of atoms that couple to each other, and its value is between 1 and N.

III. THREE-ATOM EXAMPLE

In the following, we numerically solve the resonance-spectrum of a three-atom system to demonstrate how our localization microscopy works. The dressed-state picture is

shown in Fig. 2. From Eq. (3), the eigenvalues of the system are

$$
\begin{aligned}
E_{1n} &= \left(n-\frac{3}{2}\right)\hbar\omega_0 \\
&\quad +\frac{\hbar}{2}(\Omega_1+\Omega_2+\Omega_3+\Omega_{12}+\Omega_{13}+\Omega_{23}), \\
E_{2n} &= \left(n-\frac{3}{2}\right)\hbar\omega_0 \\
&\quad +\frac{\hbar}{2}(-\Omega_1+\Omega_2+\Omega_3-\Omega_{12}-\Omega_{13}+\Omega_{23}), \\
E_{3n} &= \left(n-\frac{3}{2}\right)\hbar\omega_0 \\
&\quad +\frac{\hbar}{2}(\Omega_1-\Omega_2+\Omega_3-\Omega_{12}+\Omega_{13}-\Omega_{23}), \\
E_{4n} &= \left(n-\frac{3}{2}\right)\hbar\omega_0 \\
&\quad +\frac{\hbar}{2}(\Omega_1+\Omega_2-\Omega_3+\Omega_{12}-\Omega_{13}-\Omega_{23}), \\
E_{5n} &= \left(n-\frac{3}{2}\right)\hbar\omega_0 \\
&\quad +\frac{\hbar}{2}(-\Omega_1-\Omega_2+\Omega_3+\Omega_{12}-\Omega_{13}-\Omega_{23}), \\
E_{6n} &= \left(n-\frac{3}{2}\right)\hbar\omega_0 \\
&\quad +\frac{\hbar}{2}(-\Omega_1+\Omega_2-\Omega_3-\Omega_{12}+\Omega_{13}-\Omega_{23}), \\
E_{7n} &= \left(n-\frac{3}{2}\right)\hbar\omega_0 \\
&\quad +\frac{\hbar}{2}(\Omega_1-\Omega_2-\Omega_3-\Omega_{12}-\Omega_{13}+\Omega_{23}), \\
E_{8n} &= \left(n-\frac{3}{2}\right)\hbar\omega_0 \\
&\quad +\frac{\hbar}{2}(-\Omega_1-\Omega_2-\Omega_3+\Omega_{12}+\Omega_{13}+\Omega_{23}).
\end{aligned}
\tag{16}
$$

For weak dipole-dipole interactions, according to Eq. (12), the nonzero transition dipoles are $d_{11}^{+}=3/2$, $d_{22}^{+}=d_{33}^{+}=d_{44}^{+}=1/2, d_{55}^{+}=d_{66}^{+}=d_{77}^{+}=-1/2, d_{88}^{+}=-3/2$, $d_{12}^{-}=d_{13}^{-}=d_{14}^{-}=d_{25}^{-}=d_{26}^{-}=d_{35}^{-}=d_{37}^{-}=d_{47}^{-}=d_{58}^{-}=d_{68}^{-}=d_{78}^{-}=1/2$,and $d_{21}^{-}=d_{31}^{-}=d_{41}^{-}=d_{52}^{-}=d_{62}^{-}=d_{53}^{-}=d_{73}^{-}=d_{74}^{-}=d_{85}^{-}=d_{86}^{-}=d_{87}^{-}=-1/2$. We also can calculate $(L\rho)_{\alpha\alpha}=(3\gamma/2)\rho_{\alpha\alpha}-(\gamma/2)\sum_{\alpha'}\rho_{\alpha'\alpha'}$, where $\alpha\rightarrow\alpha'$ is the allowed sideband transition. For example, if $\alpha=1$, then $\alpha'=2,3,4$. Thus, we have

$$
\Gamma'=\frac{\gamma}{2}\begin{pmatrix}
3 & -1 & -1 & -1 & 0 & 0 & 0 & 0 \\
-1 & 3 & 0 & 0 & -1 & -1 & 0 & 0 \\
-1 & 0 & 3 & 0 & -1 & 0 & -1 & 0 \\
-1 & 0 & 0 & 3 & 0 & -1 & -1 & 0 \\
0 & -1 & -1 & 0 & 3 & 0 & 0 & -1 \\
0 & -1 & 0 & -1 & 0 & 3 & 0 & -1 \\
0 & 0 & -1 & -1 & 0 & 0 & 3 & -1 \\
0 & 0 & 0 & 0 & -1 & -1 & -1 & 3
\end{pmatrix}.
$$

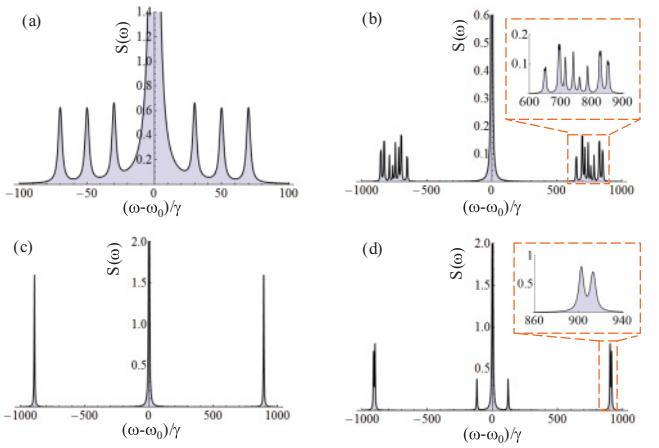

FIG. 3. (Color online) Resonance-fluorescence spectrum for (a) $x_1=0.3\lambda$, $x_2=0.5\lambda$, $x_3=0.7\lambda$, and $\Omega(x)=100\gamma x/\lambda$; (b) $x_1=0.45\lambda$, $x_2=0.5\lambda$, $x_3=0.56\lambda$, and $\Omega(x)=1500\gamma x/\lambda$; (c) $x_1=0.485\lambda$, $x_2=0.5\lambda$, $x_3=0.6\lambda$, and $\Omega(x)=1\gamma x/\lambda$; (d) same as (c) but with $\Omega(x)=200\gamma x/\lambda$.

From Eq. (9), we get the central peak spectrum,

$$
S^0(\vec{R},\omega)\propto\frac{3\gamma}{2}\left[\frac{1}{(\omega-\omega_0)^2+\gamma^2}+\frac{18}{(\omega-\omega_0)^2+4\gamma^2}+\frac{9}{(\omega-\omega_0)^2+9\gamma^2}\right]. \tag{17}
$$

For the sidebands, we numerically can solve the eigenenergy and eigenvectors of the dressed system and can calculate the allowed transition frequencies. In the real experiment, we measure the sideband peaks of the spectrum. According to Eq. (13), there are three groups of the allowed sideband spectrum on the positive side: $\omega_0+\Omega_1\pm\Omega_{12}\pm\Omega_{13}$, $\omega_0+\Omega_2\pm\Omega_{12}\pm\Omega_{23}$, and $\omega_0+\Omega_3\pm\Omega_{13}\pm\Omega_{23}$. We can obtain the Rabi frequencies for each atom by simply averaging over each group of the spectrum. For example, if we have three atoms and their positions are $x_1=0.3\lambda$, $x_2=0.5\lambda$, and $x_3=0.7\lambda$, the separation is $\lambda/5$. We shine a gradient electric field such that $\Omega(x)=100\gamma x/\lambda$. The resonance-fluorescence spectrum is shown in Fig. 3(a). From the spectrum, the sideband frequencies are $\Omega_1=(30.00\pm1.82)\gamma$, $\Omega_2=(50.00\pm1.82)\gamma$, and $\Omega_3=(70.00\pm1.72)\gamma$. We can determine the positions of the atoms as $x_1=(0.300\pm0.002)\lambda$, $x_2=(0.500\pm0.002)\lambda$, and $x_3=(0.700\pm0.002)\lambda$, which match the parameters we set very well.

As a second example, we consider that the three atoms are located at positions $x_1=0.45\lambda$, $x_2=0.5\lambda$, and $x_3=0.56\lambda$. The shortest distance is $\lambda/20$. We shine a strong gradient electric field such that $\Omega(x)=1500\gamma x/\lambda$. The resonance-fluorescence spectrum is shown in Fig. 3(b). From the spectrum, we can determine the sideband frequencies as shown in the following table (γ):

648.4 ± 2.7	715.5 ± 2.6	825.7 ± 2.7
652.4 ± 2.7	741.3 ± 2.5	829.7 ± 2.7
694.3 ± 2.8	761.5 ± 2.7	851.4 ± 2.8
698.3 ± 2.8	787.2 ± 2.5	855.3 ± 2.8

Then, we slightly increase the gradient laser field such that $\Omega(x) = 1700\gamma x/\lambda$, and the spectrum peaks are shown in the following table (γ):

693.6 ± 2.7	765.4 ± 2.6	881.7 ± 2.8
697.4 ± 2.7	791.2 ± 2.5	885.5 ± 2.8
739.5 ± 2.8	811.4 ± 2.7	907.4 ± 2.8
743.3 ± 2.8	837.2 ± 2.5	911.3 ± 2.8

Comparing these two tables, we find that the separations between peaks in each column do not change significantly. However, the separations between peaks in different columns change significantly. From this result, we can determine that the spectrum from each column belongs to same group. By averaging over each column of the first table, we can obtain $\Omega_1 = (673.35 \pm 2.75)\gamma$, $\Omega_2 = (751.38 \pm 2.58)\gamma$, and $\Omega_3 = (840.53 \pm 2.75)\gamma$. We then can determine the positions of the atoms: $x_1 = (0.449 \pm 0.002)\lambda$, $x_2 = (0.501 \pm 0.002)\lambda$, and $x_3 = (0.560 \pm 0.002)\lambda$, which also match the actual positions of the atoms quite well.

If there are two atoms whose distances are smaller than this limit, we should use the method described in Sec. II B. For example, there are three atoms, and their positions are $x_1 = 0.485\lambda$, $x_2 = 0.5\lambda$, and $x_3 = 0.6\lambda$. The distance between the first atom and the second atom is 0.015λ, which is less than $\lambda/50$. From Eq. (2), we can calculate the dipole-dipole interaction energy is 891.92γ, which is very large. In this situation, first, we apply a weak gradient laser field such that the corresponding Rabi frequency is $\Omega(x) = 1\gamma x/\lambda$. We numerically solve the resonance-fluorescence spectrum, and the result is shown in Fig. 3(c). We can see that only two sideband peaks appear, and their positions are $\omega = \omega_o \pm 891.90\gamma$, which match very well with the calculation value. From Eq. (2), we can deduce that the distance between these two close atoms is $\Delta x_{12} = 0.015\lambda$. Then, we increase the gradient laser field to a medium value, for example, $\Omega(x) = 200\gamma x/\lambda$. The numerical result of the corresponding resonance-fluorescence spectrum is shown in Fig. 3(d). From the spectrum, we find that each sideband peak is split into two peaks. For example, the positive sideband peak splits into $\omega_0 + 902.72\gamma$ and $\omega_0 + 913.36\gamma$. According to Eqs. (14) and (15), we have

$$\Omega_{12} + \frac{(\Omega_1 + \Omega_2)^2}{2\Omega_{12}} = 913.36\gamma, \tag{18}$$

$$\Omega_{12} + \frac{\Omega_1\Omega_2}{\Omega_{12}} = 902.72\gamma, \tag{19}$$

where $\Omega_{12} = 1794.84\gamma$. Assuming that $\Omega_1 = 200\gamma x_1/\lambda$ and $\Omega_2 = 200\gamma(x_1 + \Delta x_{12})/\lambda$, we can get $x_1 = 0.4816\lambda$ from Eq. (18) and $x_1' = 0.4837\lambda$ from Eq. (19). Averaging these two results, we get $\bar{x_1} = 0.483\lambda$, which is very close to the value 0.485λ we set, and the error is about 0.4%. Additionally, we find there are two sideband peaks near the central peaks that read $(\pm 120 \pm 2.6)\gamma$. They are the resonance fluorescence from the third atom, and we can determine that its position is $(0.600 \pm 0.013)\lambda$, which also matches the right value.

IV. EXTENSION TO LARGER AREA AND HIGHER DIMENSIONS

In the previous section, we discussed how to resolve the atoms located within one wavelength. For a region larger than one wavelength, one simple way is to stretch the standing wave with larger periods to cover the whole region. This method is easy to operate, but one disadvantage is that the field intensity increases as the working region increases. If the region is too large, the field is incredibly large. Therefore, for a working region beyond several wavelengths' extension, a new way may be needed. Here, we propose a possible way by trying to extend this limitation via the divide-and-conquer method. The scheme is shown in Fig. 4. We shine the sample first by a standing wave denoted by a solid and red curve. The red-marked regions on the object plane locate in an approximately linear-field region, whereas, the blue-marked regions do not. The resonance fluorescences are collected by a lens. The fluorescence emitted by the red-marked regions is focused on the red-marked detector pixels on the imaging plane, whereas, the fluorescence emitted by the blue-marked regions is focused on the blue-marked detector pixels. In this step, only the spectrum of the fluorescence collected by the red-marked detector pixels are analyzed, and we can determine the positions of the atoms in the red-marked regions on the object plane based on the method we illustrated in the previous sections. Then, we shift our standing wave by a phase $\pi/2$. At this time, the blue-marked regions locate in an approximately linear field, whereas, the red-marked regions do not. By applying a similar process, we can determine the positions of the atoms in the blue-marked regions. Because the image of a point in the object plane is not a point but a small disk, which usually is described by the point-spread function of the lens, there is a gap between neighboring detector pixels to make sure that the fluorescence from the red-marked regions does not shine on the blue-marked detector pixels and vise versa. If we have an optical detecting array for each working region on the order of several wavelengths, this method would be possible.

We also can apply our method to a 2D image. The scheme is shown in Fig. 5. Three steps are needed to obtain the 2D spatial information. In the first two steps, we shine a gradient

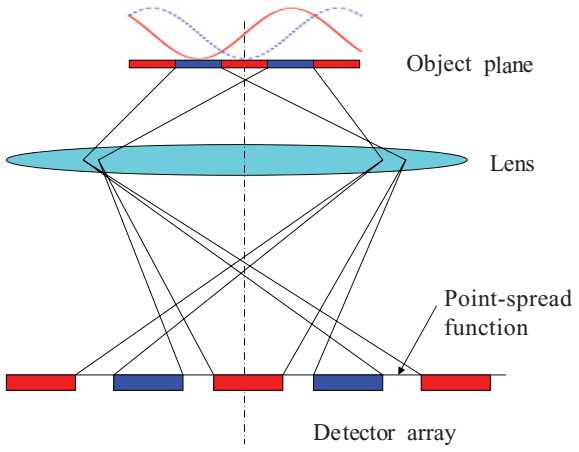

FIG. 4. (Color online) Schematic for imaging atoms in an extended region based on our RFLM.

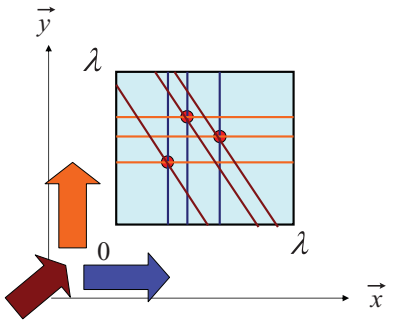

FIG. 5. (Color online) Two-dimensional RFLM.

laser field along the $x(y)$ direction, and from the resonance-fluorescence spectrum, we can obtain a discrete set of $x(y)$ position information of the atoms. After that, we still cannot determine the positions of the atoms because all combinations of x and y values are possible. We should shine a third gradient field from a direction that avoids any two pairs of (x,y). From the third resonance-fluorescence spectrum, we can pin down the positions of the atoms.

V. SUMMARY

In this paper, we evaluated the resonance-fluorescence spectrum of a bunch of two-level atoms driven by a gradient coherent laser field. In the weak dipole-dipole interaction region (separation less than $\lambda/50$), we can apply a very strong laser field such that the Rabi frequency is much larger than the dipole-dipole interaction energy. From the spectrum, we can obtain the positions of each atom by just a few measurements. Our subwavelength microscopy scheme was based entirely on a far-field technique, and it did not require point-by-point scanning, which indicated that our method may be more time efficient.

For the case in which there are two atoms that were very close to each other (less than $\lambda/50$), we still can get the position information of each atom with very high accuracy provided that they are not too close to other atoms. In addition, we illustrated a possible way to extend our method to an arbitrarily large region without requiring more peak power of the laser, and only a few measurements were required. We also briefly discussed how to image a 2D pattern.

In our scheme, uncertainty can be due to the linewidth of the spectrum and the calibration of the light intensity. Less density of atoms within $\lambda/10$ will give a narrower linewidth and, therefore, less uncertainty. Good calibration of the light intensity also was required in the experiment to extract more precise position information. There was a limitation on the number of atoms within one wavelength, which was about 50 in one dimension and 2500 in 2D space. Another limitation for our scheme was that it still was not clear how to extract the spatial information of atoms when more than two atoms were very close to each other (less than $\lambda/50$).

ACKNOWLEDGMENTS

We would like to thank Shuai Yang for helpful discussions. The research of Z.L. is supported by the Heep Fellowship. This work was supported by grants from the King Abdulaziz City for Science and Technology (KACST) and the Qatar National Research Fund (QNRF) under the NPRP Project.

APPENDIX A: EIGENVALUES AND EIGENVECTORS

The eigenvalue and eigenvector for H_0^i are

$$E_i^+ = \left(n_i - \frac{1}{2}\right)\hbar\omega_0 + \frac{\hbar\Omega_i}{2}, \qquad |\Phi_i^+\rangle = \frac{|g_i,n_i\rangle + |e_i,n_i-1\rangle}{\sqrt{2}}, \tag{A1}$$

$$E_i^- = \left(n_i - \frac{1}{2}\right)\hbar\omega_0 - \frac{\hbar\Omega_i}{2}, \qquad |\Phi_i^-\rangle = \frac{|g_i,n_i\rangle - |e_i,n_i-1\rangle}{\sqrt{2}}, \tag{A2}$$

where $\Omega_i = g\sqrt{n_i}$ and n_i is the mean number of photons interacting with the ith atom. The eigenvalues of H_0 are just the summation of the eigenvalues of each atom,

$$E_\alpha^0 = \left(n - \frac{N}{2}\right)\hbar\omega_0 + \frac{\hbar}{2}\sum_i \chi_i^\alpha \Omega_i, \tag{A3}$$

where $\alpha = 1,2,\ldots,2^N$, $n = \sum_i n_i$, and $\chi_i^\alpha = \pm 1$. The corresponding eigenvectors are

$$|\alpha\rangle = \frac{1}{\sqrt{2^N}}\bigotimes_{i=1}^{N}(|g_i,n_i\rangle + \chi_i^\alpha|e_i,n_i-1\rangle), \tag{A4}$$

which is equivalent to Eq. (2).

The perturbation energy due to the dipole-dipole interaction is

$$\begin{aligned}
\Delta_\alpha &= \langle\alpha|H_{dd}|\alpha\rangle \\
&= \hbar\sum_{i\neq j}\Omega_{ij}\langle\alpha|S_i^+S_j^- + S_j^+S_i^-|\alpha\rangle \\
&= \frac{\hbar}{4}\sum_{i\neq j}\Omega_{ij}\big(\langle g_i| + \langle e_i|\chi_i^\alpha\big)\big(\langle g_j| + \langle e_j|\chi_j^\alpha\big) \\
&\quad\times(S_i^+S_j^- + S_j^+S_i^-)\big(|g_i\rangle + \chi_i^\alpha|e_i\rangle\big)\big(|g_j\rangle + \chi_j^\alpha|e_j\rangle\big) \\
&= \frac{\hbar}{4}\sum_{i\neq j}\Omega_{ij}\big(\langle g_i| + \langle e_i|\chi_i^\alpha\big)\big(\langle g_j| + \langle e_j|\chi_j^\alpha\big) \\
&\quad\times\big(\chi_j^\alpha|e_i\rangle|g_j\rangle + \chi_i^\alpha|g_i\rangle|e_j\rangle\big) \\
&= \frac{\hbar}{2}\sum_{i\neq j}\chi_i^\alpha\chi_j^\alpha\Omega_{ij},
\end{aligned} \tag{A5}$$

where we have ignored the photon part because the dipole-dipole Hamiltonian only depends on atomic operators.

APPENDIX B: LINEWIDTH

Assume that $|\alpha\rangle \to |\beta\rangle$ is an allowed transition, i.e., $\alpha = \beta$, or they differ from each other by only one term. The relaxation

term for the $|\alpha\rangle \to |\beta\rangle$ transition is given by

$$(L\rho)_{\alpha\beta} = \sum_{i,j=1}^{N} \gamma_{ij}(\langle\alpha|S_i^+ S_j^- \rho|\beta\rangle + \langle\alpha|\rho S_i^+ S_j^-|\beta\rangle - 2\langle\alpha|S_j^- \rho S_i^+|\beta\rangle). \tag{B1}$$

For $i = j$, we have

$$S_i^+ S_i^-|\alpha\rangle = \frac{1}{\sqrt{2^N}} \bigotimes_{k\neq i} \left(|g_k\rangle + \chi_k^\alpha |e_k\rangle\right)\left(\chi_i^\alpha |e_i\rangle\right) = \frac{1}{2}(|\alpha\rangle - |\alpha^i\rangle), \tag{B2}$$

$$S_i^+ S_i^-|\beta\rangle = \frac{1}{\sqrt{2^N}} \bigotimes_{k\neq i} \left(|g_k\rangle + \chi_k^\beta |e_k\rangle\right)\left(\chi_i^\beta |e_i\rangle\right) = \frac{1}{2}(|\beta\rangle - |\beta^i\rangle), \tag{B3}$$

$$S_i^+|\alpha\rangle = \frac{1}{\sqrt{2^N}} \bigotimes_{k\neq i} \left(|g_k\rangle + \chi_k^\alpha |e_k\rangle\right)|e_i\rangle = \chi_i^\alpha \frac{|\alpha\rangle - |\alpha^i\rangle}{2}, \tag{B4}$$

$$S_i^+|\beta\rangle = \frac{1}{\sqrt{2^N}} \bigotimes_{k\neq i} \left(|g_k\rangle + \chi_k^\beta |e_k\rangle\right)|e_i\rangle = \chi_i^\beta \frac{|\beta\rangle - |\beta^i\rangle}{2}, \tag{B5}$$

where $|\alpha^i\rangle$ and $|\alpha\rangle$ have different signs only on the ith term and $|\beta^i\rangle$ and $|\beta\rangle$ have different signs on the ith term. There are $N-1$ pairs that satisfy this condition. From Eqs. (B2)–(B5), we can get

$$\begin{aligned}\sum_i \gamma_{ii}(&\langle\alpha|S_i^+ S_i^- \rho|\beta\rangle + \langle\alpha|\rho S_i^+ S_i^-|\beta\rangle - 2\langle\alpha|S_i^- \rho S_i^+|\beta\rangle) \\ &= \frac{\gamma}{2}\sum_i \left\{\left[2 - \chi_i^\alpha \chi_i^\beta\right]\rho_{\alpha\beta} - \left[1 - \chi_i^\alpha \chi_i^\beta\right]\rho_{\alpha^i\beta} \right. \\ &\quad \left. - \left[1 - \chi_i^\alpha \chi_i^\beta\right]\rho_{\alpha\beta^i} - \chi_i^\alpha \chi_i^\beta \rho_{\alpha^i\beta^i}\right\}, \end{aligned} \tag{B6}$$

$$= \begin{cases} \dfrac{N\gamma}{2}\rho_{\alpha\beta} - \dfrac{\gamma}{2}\displaystyle\sum_i \rho_{\alpha^i\beta^i}, \\ \dfrac{(N+2)\gamma}{2}\rho_{\alpha\beta} - \dfrac{\gamma}{2}\displaystyle\sum_i \rho_{\alpha^i\beta^i} - \rho_{\beta\alpha} - 2\rho_{\beta\beta} - 2\rho_{\alpha\alpha}, \end{cases} \tag{B7}$$

in which the first equation in Eq. (B7) is for $\alpha = \beta$, whereas, the second equation is for $\alpha \neq \beta$ but only differs by one term. The last three terms in the second equation can be ignored in the secular approximation because they have different transition frequencies from $\omega_{\alpha\beta}$. The survival of the second term depends on the coupling of the system. If all dipole-dipole interaction energies are small and can be neglected, the second term survives because $\omega_{\alpha^i\beta^i} = \omega_{\alpha\beta}$ and there are $N-1$ terms. When we repeat the calculation of Eq. (B6) for other transitions, we can find that $\rho_{\alpha\beta}$ appears one time with coefficient $(N+2)\gamma/2$ and $N-1$ times with coefficient $-\gamma/2$. Therefore, when we perform the summation over the whole set, we can find the coefficient of $\rho_{\alpha\beta}$ is $(N+2)\gamma/2 - (N-1)\gamma/2 = 3\gamma/2$, which is exactly the linewidth of the independent atoms. However, if all dipole-dipole interactions cannot be neglected, then the second term goes away in the secular approximation due to $\omega_{\alpha^i\beta^i} \neq \omega_{\alpha\beta}$, and the linewidth in this case is $(N+2)\gamma/2$.

In Eq. (B1), we also have correlated spontaneous emission terms ($i \neq j$). These terms appear only when the dipole-dipole interaction cannot be neglected. We consider an extreme case when all dipole-dipole interactions cannot be neglected and no spectrum is overlapped. In this case, we have

$$S_j^+ S_i^-|\alpha\rangle = \frac{1}{\sqrt{2^N}} \bigotimes_{k\neq i,j} \left(|g_k\rangle + \chi_k^\alpha |e_k\rangle\right)\left(\chi_i^\alpha |g_i\rangle\right)|e_j\rangle = \frac{1}{4}\chi_i^\alpha \chi_j^\alpha |\alpha\rangle + \cdots, \tag{B8}$$

$$S_i^+ S_j^-|\beta\rangle = \frac{1}{\sqrt{2^N}} \bigotimes_{k\neq i,j} \left(|g_k\rangle + \chi_k^\beta |e_k\rangle\right)|e_i\rangle\left(\chi_j^\beta |g_j\rangle\right) = \frac{1}{4}\chi_i^\beta \chi_j^\beta |\beta\rangle + \cdots, \tag{B9}$$

$$S_j^+|\alpha\rangle = \frac{1}{\sqrt{2^N}} \bigotimes_{k\neq j} \left(|g_k\rangle + \chi_k^\alpha |e_k\rangle\right)|e_j\rangle) = \frac{\chi_i^\alpha}{2}|\alpha\rangle + \cdots, \tag{B10}$$

$$S_i^+|\beta\rangle = \frac{1}{\sqrt{2^N}} \bigotimes_{k\neq i} \left(|g_k\rangle + \chi_k^\beta |e_k\rangle\right)|e_i\rangle = \frac{\chi_i^\beta}{2}|\beta\rangle + \cdots, \tag{B11}$$

where $\cdots$ denote terms that have different transition frequencies from $\omega_{\alpha\beta}$ and they can be neglected in the secular approximation. Then, we can have

$$\begin{aligned}\sum_{i\neq j} \gamma_{ij}(&\langle\alpha|S_i^+ S_j^- \rho|\beta\rangle + \langle\alpha|\rho S_i^+ S_j^-|\beta\rangle - 2\langle\alpha|S_j^- \rho S_i^+|\beta\rangle) \\ &= \sum_{i\neq j} \frac{\gamma_{ij}}{4}\left[\chi_i^\alpha \chi_j^\alpha + \chi_i^\beta \chi_j^\beta - 2\chi_j^\alpha \chi_i^\beta\right]\rho_{\alpha\beta} + \cdots \\ &= \left\{ \sum_{i\neq j\neq p} \frac{\gamma_{ij}}{4}\left[\chi_i^\alpha \chi_j^\alpha + \chi_i^\beta \chi_j^\beta - 2\chi_j^\alpha \chi_i^\beta\right] \right. \\ &\quad + \sum_{j\neq p} \frac{\gamma_{pj}}{4}\left[\chi_p^\alpha \chi_j^\alpha + \chi_p^\beta \chi_j^\beta - 2\chi_j^\alpha \chi_p^\beta\right] \\ &\quad \left. + \sum_{i\neq p} \frac{\gamma_{ip}}{4}\left[\chi_i^\alpha \chi_p^\alpha + \chi_i^\beta \chi_p^\beta - 2\chi_p^\alpha \chi_i^\beta\right]\right\}\rho_{\alpha\beta} + \cdots \\ &= 0. \end{aligned} \tag{B12}$$

The first summation vanishes because $\chi_i^\alpha = \chi_i^\beta$ and $\chi_j^\alpha = \chi_j^\beta$ for $i, j \neq p$. Because $\chi_p^\alpha = -\chi_p^\beta$ and $\chi_j^\alpha = \chi_j^\beta$, the first two terms in the second summation go away. Similarly, the first two terms of the third summation also go away. The remaining terms in the second and third summations are just

the opposite because

$$\sum_{j\neq p}\frac{\gamma_{pj}}{4}\left[-2\chi_j^{\alpha}\chi_p^{\beta}\right]=\sum_{i\neq p}\frac{\gamma_{pi}}{4}\left[-2\chi_i^{\alpha}\chi_p^{\beta}\right]$$
$$=\sum_{i\neq p}\frac{\gamma_{pi}}{4}\left[+2\chi_i^{\beta}\chi_p^{\alpha}\right]. \quad \text{(B13)}$$

When we consider the first-order correction of the wave function, this correlated spontaneous emission rate is nonzero. However, their values are on the order of $(\Omega_{ij}/\Omega_i)^2$, which is very small in our assumption.

[1] E. Abbe, Arch. Mikr. Anat. **9**, 413 (1873).
[2] L. Rayleigh, Philos. Mag. **47**, 81 (1874).
[3] *Nanoscopy and Multidimensional Optical Fluorescence Microscopy*, edited by A. Diaspro (CRC, Boca Raton, 2010).
[4] G. Binnig, C. F. Quate, and C. Gerber, Phys. Rev. Lett. **56**, 930 (1986).
[5] C. Hettich *et al.*, Science **298**, 385 (2002).
[6] W. Denk, J. H. Strickler, and W. W. Webb, Science **248**, 73 (1990).
[7] J. H. Strickler and W. W. Webb, Proc. SPIE **1398**, 107 (1991).
[8] S. W. Hell and J. Wichmann, Opt. Lett. **19**, 780 (1994).
[9] S. W. Hell and M. Kroug, Appl. Phys. B **60**, 495 (1995).
[10] T. A. Klar and S. W. Hell, Opt. Lett. **24**, 954 (1999).
[11] E. Rittweger, K. Y. Han, S. E. Irvine, C. Eggeling, and S. W. Hell, Nat. Photonics **3**, 144 (2009).
[12] G. S. Agarwal and K. T. Kapale, J. Phys. B **39**, 3437 (2006).
[13] S. Bretschneider, C. Eggeling, and S. W. Hell, Phys. Rev. Lett. **98**, 218103 (2007).
[14] D. D. Yavuz and N. A. Proite, Phys. Rev. A **76**, 041802(R) (2007).
[15] A. V. Gorshkov, L. Jiang, M. Greiner, P. Zoller, and M. D. Lukin, Phys. Rev. Lett. **100**, 093005 (2008).
[16] M. Kiffner, J. Evers, and M. S. Zubairy, Phys. Rev. Lett. **100**, 073602 (2008).
[17] H. Li, V. A. Sautenkov, M. M. Kash, A. V. Sokolov, G. R. Welch, Y. V. Rostovtsev, M. S. Zubairy, and M. O. Scully, Phys. Rev. A **78**, 013803 (2008).
[18] Z. Liao, M. Al-Amri, and M. Suhail Zubairy, Phys. Rev. Lett. **105**, 183601 (2010).
[19] C. Shin *et al.*, J. Lumin. **130**, 1635 (2010).
[20] I. Gerhardt, G. Wrigge, J. Hwang, G. Zumofen, and V. Sandoghdar, Phys. Rev. A. **82**, 063823 (2010).
[21] J-T. Chang, J. Evers, M. O. Scully, and M. S. Zubairy, Phys. Rev. A **73**, 031803(R) (2006).
[22] Q. Sun, M. Al-Amri, M. O. Scully, and M. S. Zubairy, Phys. Rev. A **83**, 063818 (2011).
[23] T. G. Rudolph, Z. Ficek, and B. J. Dalton, Phys. Rev. A **52**, 636 (1995).
[24] G. Lenz and P. Meystre, Phys. Rev. A **48**, 3365 (1993).
[25] Z. Ficek and S. Swain, *Quantum Interference and Quantum Coherence: Theory and Experiment* (Springer, New York, 2004).
[26] C. Cohen-Tannoudji and S. Reynaud, J. Phys. B **10**, 345 (1977).
[27] H. S. Freedhoff, Phys. Rev. A **19**, 1132 (1979).
[28] M. O. Scully and M. S. Zubairy, *Quantum Optics* (Cambridge University Press, Cambridge, UK, 1997).
[29] R. H. Dicke, Phys. Rev. **93**, 99 (1954).